Gabor Wavelets for 3-D Object Recognition

Xing Wu and Bir Bhanu

College of Engineering
University of California, Riverside, CA 92521-0425
Email: xingwu@constitution.ucr.edu, bhanu@shivish.ucr.edu

Abstract

This paper presents a model-based object recognition approach that uses a hierarchical Gabor wavelet representation. The key idea is to use magnitude, phase and frequency measures of Gabor wavelet representation in an innovative flexible matching approach that can provide robust recognition. A Gabor grid, a topology-preserving map, efficiently encodes both signal energy and structural information of an object in a sparse multi-resolution representation. The Gabor grid subsamples the Gabor wavelet decomposition of an object model and is deformed to allow the indexed object model match with the image data. Flexible matching between the model and the image minimizes a cost function based on local similarity and geometric distortion of the Gabor grid. Grid erosion and repairing is performed whenever a collapsed grid, due to object occlusion, is detected. The results on infrared imagery are presented, where objects undergo rotation, translation, scale, occlusion and aspect variations under changing environmental conditions.

1 Introduction

Model-based object recognition in real-world outdoor situations is difficult because a robust algorithm has to consider multiple factors such as, object contrast, signature, scale, and aspect variations; noise and spurious low resolution sensor data; and high clutter, partial object occlusion and articulation. Current approaches use shape primitives, silhouette and contours, colors, and invariant object features for matching. The performance of these methods is acceptable when objects are well defined, have high contrast, and are at close ranges. However, these approaches do not gracefully degrade and produce high false alarms when competitive clutter and object shape distortion are present in the input data. To improve the performance under multi-scenarios and varying environmental conditions, model of sensors, atmosphere, and background clutter are helpful in addition to the geometric model of an object. Using only a minimum set of models and sensor model, multi-scale Gabor representation and a flexible matching mechanism described in the paper can help to improve the recognition performance under real-world situations.

The goal of the research presented in this paper is to recognize 3D rigid objects in cluttered multisensor images with varying appearances, signatures and possible partial occlusion using a model-based paradigm.

2 Our Approach

The general scheme of our system is depicted in Figure 1. It is implemented as an iterative process of matching by first finding the optimal global placement of the grid over a region-of-interest of the object while the grid is kept rigid (*location indexing*), then deformation of the grid allows model Gabor probes match with local features of the distorted image (*flexible matching*). Gabor magnitude is used in probe matching based on local structural energy patterns. Gabor frequency is used to estimate the scale variation of a given object from the model. Gabor phase is used to evaluate the matching result in terms of average local image displacement between the model and the data, and support interpolation between aspects of the model.

In our work, 3D objects are represented by a series of viewer-centered 2D images of the objects at various aspect and depression angles, $\mathcal{M} = \{M_1, M_2, \ldots, M_K\}$, called object aspects. These models are generated offline. Both object and object model are represented by the magnitude and
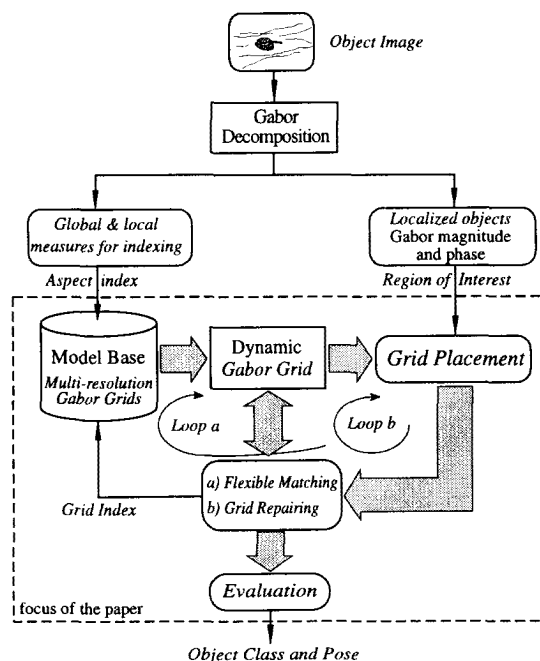
Figure 1: Our object recognition approach.

phase responses of multi-scale Gabor wavelet filters. Objects are recognized when they successfully match with a specific model based on distinctive local features in the Gabor wavelet representation.

The most closely related work to our approach is Lades's "Dynamic Link Architecture" technique [4]. The key differences between our approach and Lades's techniques are given in [1]. The main contribution of this paper is to use Gabor wavelet representation to recognize 3-D objects under scale, aspect and significant distortions in shape and appearance, due to changing environmental conditions.

2.1 Gabor Function and Gabor Wavelets

The general form of a 2D Gabor function is given as [2],

$$G(x,y) = \exp\left\{-\pi[(\frac{x'}{\sigma})^2 + (\frac{y'}{\alpha\sigma})^2]\right\} \cdot$$
$$\exp\left\{j\left[u\left(x - x_i\right) + v\left(y - y_i\right)\right]\right\}, \quad (1)$$

$$u = \omega_k \cos\theta_l, \quad v = \omega_k \sin\theta_l.$$
$$\left[\begin{array}{c} x' \\ y' \end{array}\right] = \left[\begin{array}{cc} \cos\phi_G & \sin\phi_G \\ -\sin\phi_G & \cos\phi_G \end{array}\right]\left[\begin{array}{c} x - x_i \\ y - y_i \end{array}\right]$$

In the above formula, (x_i, y_i) is the spatial centroid of the elliptical Gaussian window whose scale and aspect are regulated by σ and α, respectively. ω_k and θ_l are the modulation frequency and direction, and (u, v) are frequency components of ω_k in x and y directions, respectively. The scale σ controls the size of the filter as well as its bandwidth, while the aspect ratio α and the rotation parameter ϕ_G control the shape of the spatial window and the spectral channel passband and is generally set equal to θ_l.

By representing Gabor wavelet filters as a propagated quadrature pair $\langle G_\psi^+, G_\psi^- \rangle$, a representation which is similar to the so called wavelet [5] is defined. The log-polar sampling in the frequency domain generated by the 2D wave propagation vector $\vec{\psi}$ is given as:

$$\vec{\psi}_{\omega_k,\theta_l} = \omega_k \cdot e^{i\theta_l}, \quad where \quad \omega_k = \rho^k \cdot \omega_0, \quad and \quad \theta_l = l \cdot \theta_0. \quad (2)$$

Also, the modulation frequency increases proportionally with the reduction in scale,

$$\sigma_k = \frac{1}{\rho}\sigma_{k-1}, \quad \omega_k = \rho\omega_{k-1}. \quad (3)$$

Therefore, the wavelet filter kernel's frequency and orientation bandwidth are defined as:

$$\Delta\omega_k = \lambda\omega_k, \quad \Delta\theta_l \approx \lambda. \quad (4)$$

whereλ is called bandwidth-frequency ratio.

The Gabor wavelet decomposition of an object image $I(\mathbf{x})$ is an iconic multi-resolution template. To reduce the inter-pixel redundancy, subsampling this template forms an elastic Gabor grid $\mathcal{G}_D$ which covers the whole object with $N \times M$ nodes (vertices V_i and edges E_j) in the x and y directions, respectively, $\mathcal{G}_D = \langle V_m, E_n \rangle$.

Each node $v_k \in V_m$ is a triple, $v_j = \langle \mathbf{x}_j, P_j^+, P_j^- \rangle$ where $\mathbf{x}_j$ is the image coordinates of grid node j (with respect to some normalized coordinate frame). Nodes are selected with fixed distance D_{space} from neighboring nodes for a model
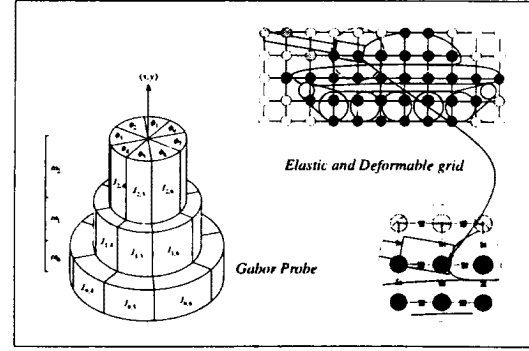
Figure 2: Gabor probe and grid

grid, $\mathbf{x}_j = (x_0 + nD_{space}, y_0 + mD_{space})$. P_j is a vector of length $K \times L$ which is referred to as a Gabor probe,

$$P_j^+[k, l] = (I * G_{\psi_{k,l}}^+)[\mathbf{x}_j],$$
$$P_j^-[k, l] = (I * G_{\psi_{k,l}}^-)[\mathbf{x}_j]. \quad (5)$$

where $(G_{\psi_{k,l}}^+, G_{\psi_{k,l}}^-)$ is a Gabor wavelet quadrature filter pair with center frequency ω_k and modulation orientation ϕ_l. The role of the graph edges $e_{i,j} \in E_n$ is to represent neighborhood relationships and serve as constraint during matching, where they are interpreted as elastic links. An edge can be deformed like a spring to make a model probe match with the Gabor decomposition of a distorted object. The length between two nodes $d_{ij} = \|x_i - x_j\|$ and grid angle attached to that edge serve as initial constraints. Thus, current distortions can be measured and penalized immediately during matching.

Figure 2 shows the Gabor grid and Gabor probe representation. The extracted information (both signal energy and local pattern structure) associated with each probe spans a neighborhood whose size equals the extent of the filter kernel.

3 Object Recognition—Flexible Matching

The flexible matching for object recognition process includes (1) *Grid placement* to find the location and index of an object in an input image; (2) *Flexible matching* to fine tune the object aspect according to the object distortion present in the input data; and (3) *Evaluation* to select the best matched aspect by following the selected rules. Grid repairing is performed when object is occluded.

3.1 Location Indexing

At this stage of the matching process, the indexed aspect Gabor grid G_{idx} that potentially corresponds to the object aspect A_{idx} is positioned ($\mathbf{x}_{idx}$), scaled (s_{idx}), and rotated (ϕ_{idx}), according to the index elements while the grid is kept rigid,

$$G_{idx} = \langle V_{idx}, E_{idx} \rangle \xrightarrow{\mathbf{X},s,\phi} G'_{idx} = \langle V'_{idx}, E'_{idx} \rangle$$

where

$$v'_j = \langle \mathbf{x} + S_{s,\phi}(\mathbf{x}_j), S_{s,\phi}(P_j^+), S_{s,\phi}(P_j^-) \rangle$$
$$e'_{i,j} = s \cdot d_{i,j} \quad (6)$$

for all $v_j \in V_{idx}$ and $e_{i,j} \in E_{idx}$. The function $S_{s,\phi}()$ performs scaling and rotation operations on the grid nodes.

When the scale factor s is a power of ω_0 and the orientation ϕ is a multiple of ϕ_0, it corresponds to deriving a new model grid $\mathcal{G}'_D$ at a given scale by scaling down edges of the Gabor grid by factor s, and shifting and rotating Gabor probe P_j at each node v_j from the corresponding frequency index ω_s and orientation ϕ_s.

$$\begin{cases} e_j & \mapsto & e_j/(\sqrt{2})^s, \\ P_j(\omega_k, \phi_l) & \mapsto & P_j(\omega_{(k-s)}, \phi_{l-s}). \end{cases} \quad (7)$$

In case s is not a multiple of ρ or ϕ is a *not* a power of Δ_ϕ, we can either, (a) round the scale factor s to s' which is the closest multiple of the frequency index ρ in (7), and let the subsequent flexible matching overcome this small scale distortion in Gabor decomposition. However, the grid edge will be scaled according to the exact scale factor s. or, (b) implement a suitable interpolation scheme over scale and orientation.

The object decomposition by a Gabor filter at a specific frequency corresponds to an object representation at a specific scale. By comparing the similarities of these representations between an object and a model grid, it allows to estimate the object scale.

3.2 Flexible Model Matching

After location indexing, flexible matching starts to further verify the hypothesis for a model aspect by moving nodes of the model Gabor grid locally and independently to find the best matched image probes. In this process, the $2D$ images of an object corresponding to two viewing aspects (with small aspect difference) is simulated by "small local" elastic deformations of one of the objects.

When the external forces are applied, an elastic object is deformed until an equilibrium state between the external forces and internal forces resisting the deformation is achieved. This equilibrium state can be described as,

$$\mu \nabla^2 \mathbf{u} + (\gamma + \mu)\frac{\partial \mathbf{u}}{\partial \mathbf{x}} + \mathbf{F} = 0, \quad (8)$$

where $\mathbf{x}$ is the coordinate of the object, $\mathbf{u}$ is the displacement of the deformation, $\mathbf{F}$ is the external forces, and μ and γ define the elastic properties of the object. To find the equilibrium state when the deformable model grid is matched with an object decomposition, equation (8) is formatted as an iterative process which minimizes a cost function $\mathcal{C}$ balanced between grid distortions $\mathcal{D}$ and local similarities $\mathcal{S}$. Therefore, we can rewrite (8) as following,

$$\mathcal{C} = \mu \sum_i^N \mathcal{D}(v_i) - \sum_i^N \mathcal{S}(P_i^I, P_i^M), \quad (9)$$

where N is the total number of grid nodes, μ is the elastic parameter which controls the grid deformation. v_i is a grid vertex, and P^I and P^M are the object Gabor decomposition and a model Gabor probe, respectively. $\mathcal{D}$ and $\mathcal{S}$ are defined by equation (12) and (13), respectively.

Flexible Matching Algorithm

1. Use the index generated by the grid-placement algorithm as the initial placement of the model grid.

(a) Model image   (b) Object image

(c) Matching result   (d) Projected model
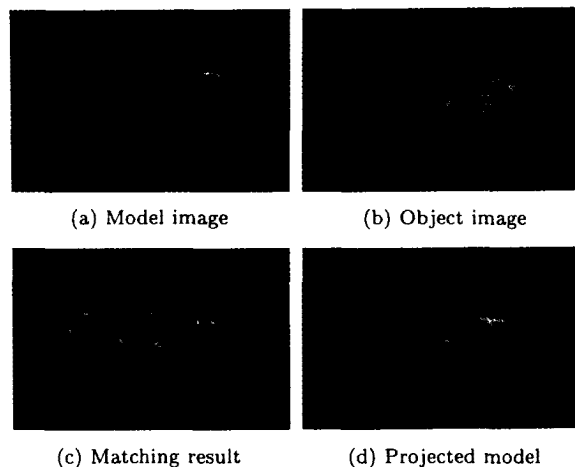
Figure 3: Illustration of the quality of flexible matching

2. For each grid node (visited in random order), take a random step s. A move s for a node is valid and can be accepted if either,

   - the global cost $\mathcal{C}$ is reduced due to this move, or
   - $\Delta\mathcal{C}$ satisfies a probability $\exp(-\Delta\mathcal{C}/T)$, where T is the annealing temperature.

3. The matching terminates and produces a deformed model grid if either the matching reaches a desired cost, or the annealing temperature is freezing. If neither condition is satisfied, continue previous step with temperature decreased by a cooling factor β.

4. Compute the similarity between the distorted model grid and the object Gabor decomposition, the deformation of the model grid, and the Gabor phase-based matching error (see section 3.5).

To show the quality of flexible matching under distortions, an example is given in Figure 3, in which a matched model is *back projected* onto the object image using the transformation which is calculated based on the relationship between the model grid and the matched deformed grid, and bilinear interpolation for gray scale values. The pose of the object is also derived in this manner.

3.3 Evaluation of Matching

The process of matching always yields a best value for C in (9) regardless of whether or not a corresponding object is in the model database. Successful recognition tends to have small geometric distortions and high similarity measurements. However, a matching result for the correct object class may not be distinctive when large object aspect variations and large changes in object signatures are present in the input data. To overcome the drawbacks of using only a single evaluation criterion, we introduce a set of comprehensive measures.

1. *Flexible matching cost* ς : It is given by (9), ς combines the similarity measure between probes and grid distortions. To suppress background probes and compensate for grid deformation, the similarity measure term is mul-

tiplied by the minimum magnitude of either the model or the object probe.

2. *Dissimilarity* ε : It is defined as the difference between perfect matching and the actual matching results. ε is zero for perfectly matched probes, and is less than 0.5 for a randomly matched probe pair.

$$\varepsilon = \sum_{i}^{N} \left[1 - \bar{S}(P_i^I, P_i^M)\right]^2 , \qquad (10)$$

where $\bar{S}$ is given by equation (13)

3. *Displacement* δ : It is defined as the local translational displacement between matched Gabor probes. Given that a model probe P_m matches with an image probe P_i, the localized phase difference along the direction of modulation ϕ_l for a specific filter frequency ω_k can be used to estimate this displacement and evaluate the matching error,

$$d(\omega_k, \phi_l) = \frac{\Delta\theta(\omega_k, \phi_l)}{\omega_k} \qquad (11)$$

To find the correct object aspect after flexible matching, the results are evaluated based on the three criteria discussed above and the following rules in order.

1. For all matching results, sort the ς, ε and *delta* in descending order.

2. Select the model having both the lowest matching cost ς and the smallest dissimilarity ε. If neither the values of ς or ε for the top two matched models are distinguishable enough (by a predefined threshold), go to Step 4.

3. Select the model having the smallest dissimilarity ε while its matching cost ς and dissimilarity ε are both lower than a predefined threshold.

4. Select the model having the smallest displacement measure which is less than a predefined threshold.

5. Any matches which fail the above tests are rejected for recognition.

In a separate experiment to recognize 138 objects [1], a success rate of 61.8% was achieved when only the flexible matching cost is used in matching. The performance is improved by using other evaluation criteria, and a successful recognition rate of 98% was achieved when the three described evaluation criteria are used together (see Table 1).

Table 1: Statistics of recognition performance for a total of 207 images. (ς: final matching cost, ε: dissimilarity measurement, δ: phase based average image displacement.)

Criteria	Images	Failures	Recognition Performance
ς	207	79	61.8%
$\varsigma + \varepsilon$	207	14	93.2%
$\varsigma + \varepsilon + \delta$	207	5	97.6%

3.4 Computational Issues

The distortion of the grid is computed to represent the distortion of a 2D image due to the aspect changes of a 3D object. To precisely estimate the deformation of a 2D image by a Gabor grid, *length* and *angular* distortion are defined by
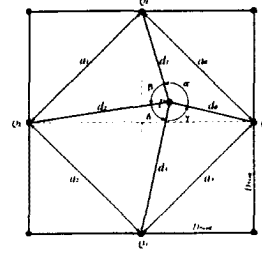
Figure 4: Illustration of grid deformation

comparing the current grid with its original structure which has fixed length and a rectilinear grid. The distortion for a node v_k is then calculated as:

$$\mathcal{D}(v_k) = \sum_{i=0}^{3} (d_i - D_{fixed})^2 + \sum_{i=0}^{3} \left(a_i - \sqrt{d_i^2 + d_{i+1}^2}\right)^2 \quad (12)$$

The first term in (12) measures the grid length distortion, while the second term measures the angular distortion.

Given each Gabor probe as a *vector* of Gabor wavelet decomposition of magnitude at a spatial location, to match local features between two objects corresponds a search of maximum similarity between a model Gabor probe and an image probe. The similarity between two Gabor probes is computed as follow:

$$\bar{S}(\vec{P}, \vec{Q}) = \frac{1}{\eta} \frac{\vec{P} \cdot \vec{Q}}{\|\vec{P}\| \cdot \|\vec{Q}\|} \min\left(\frac{\|\vec{P}\|}{\|\vec{Q}\|}, \frac{\|\vec{Q}\|}{\|\vec{P}\|}\right) , \qquad (13)$$

where η is a normalization term that is used to reduce the effect of object signature variations. In practice, we choose η to be the following:

$$\eta = \min\left(\frac{\|\vec{J}_p\|}{\|\vec{J}_q\|}, \frac{\|\vec{J}_q\|}{\|\vec{J}_p\|}\right) \quad \vec{J}_p = \{\vec{J}_k : \max(\frac{\vec{J}_k \cdot \vec{J}_i}{\|\vec{J}_k\| \cdot \|\vec{J}_i\|}), \forall k\} .$$
$$(14)$$

3.5 Gabor Phase based Evaluation

Assume that the matched model and object image are locally similar to each other only when a small shift Δx is made. Due to the fact that a shift of an image in the spatial domain corresponds to a phase shift in the frequency domain (Fourier transform), then, in that region we can estimate this shift Δx by $\Delta\phi/\omega_k$. It is approximately true for Gabor filters under certain conditions [6, 3]. Therefore, it allows far more precise model/object alignment by using Gabor phase information.

The phase difference at center frequency ω_k and orientation ϕ_l between a model and an image probe is given as,

$$\Delta\theta(\omega_k, \phi_l) = \theta_m(\omega_k, \phi_l) - \theta_i(\omega_k, \phi_l)$$
$$= \tan^{-1}\left(\frac{a_m^-(\omega_k, \phi_l)a_i^+(\omega_k, \phi_l) - a_m^+(\omega_k, \phi_l)a_i^-(\omega_k, \phi_l)}{a_m^-(\omega_k, \phi_l)a_i^-(\omega_k, \phi_l) + a_m^+(\omega_k, \phi_l)a_i^+(\omega_k, \phi_l)}\right)$$

where a^+ and a^- are the *cosine* and *sine* Gabor probes respectively. Thus, the translational displacement in the direction of ϕ_l can be estimated as (11). To overcome noise using all available filter bands, the displacement estimates for a probe by different filter frequency bands and orientations are averaged [1].

(a) Model (67.5° aspect)   (b) Object (50° aspect)

(c) Matching error   (d) Projected model
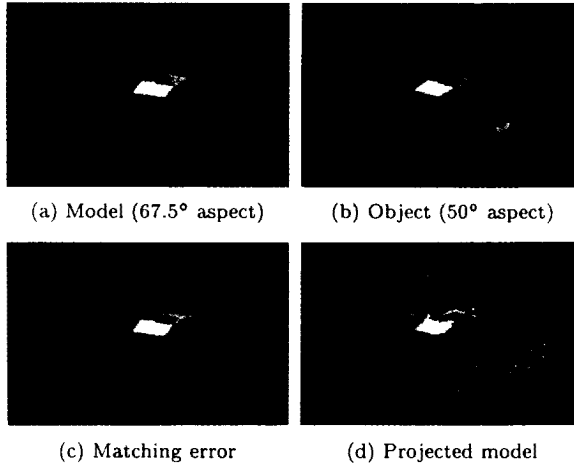
Figure 5: Illustration of phased based evaluation.

Due to the observation that grid nodes are not necessarily located at high Gabor magnitude response points, in our approach, points selected from the object with high Gabor magnitude responses are used and back-projected onto the matched model. An average of the amplitude of the local displacement estimated for all these points is used as the matching error δ for comparison. More accurate phase measures can be obtained using these projected pairs than using grid nodes.

Figure 5 gives a quantitative illustration of how phase based evaluation is used to estimate matching error. In this example, the aspect of the object and the model are 50° and 67.5° respectively. Points selected from the object image (Figure 5(b)), which are local high Gabor magnitude responses, are back projected onto the matched model (Figure 5(a)) using the transformation computed by the matched deformed Gabor grid. The matching errors estimated for each of these points in terms of local image displacement is displayed by their direction and magnitude in Figure 5(c). An average local image displacement of 3.4 pixels is measured in this example.

3.6 Recognizing Occluded Objects

Our approach for recognizing an occluded object can be described by *dynamic modification* of the Gabor grid through grid erosion and repairing processes performed during matching. The idea is to determine which subset of the Gabor grid matches with the non-occluded part of the object. Since a Gabor grid encodes the localized signal energy and structural patterns of an object, following two facts can be used to detect a potentially occluded object,

1. During matching, any collapsed grid results due to object occlusion.

2. A sub-Gabor grid corresponding to the occluded part has very low similarity measurement (≤ 0.3) due to random matching with background clutter.

Thus, it is safe to assume that the part of the grid having a non-collapsed grid and high similarity matching result corresponds to the non-occluded part of the object. Grid nodes

from the hypothesized occluded part of the Gabor grid are discarded iteratively during dynamic grid refinement. The following processes are repeated until no more refinement is necessary: (1) *location indexing*, (2) *flexible matching*, and (3) *grid repairing*. (See loop b in Figure 1).

Grid Repairing Algorithm

1. Detect collapsed and randomly matched results using following facts:
   - a collapsed grid nodes can be detected by examining the relationship between the corresponding nodes in the connected and the complementary grid.
   - grid nodes which randomly matched with background clutter will have lower similarity measurement (less than 0.3). When a column or several columns of grid nodes have random matching results, they are marked as potential occluded object grid nodes.

2. Create the connected and complementary grids. Find and mark the collapsed grid nodes in both graphs.

3. Remove collapsed grid nodes and corresponding edges according to their spatial locations and relationships.

4. Remove isolated subgrids (nodes).

5. Remove subgrids that have similarity measures lower than a threshold due to the random matching with the background clutter.

6. Reevaluate matching result based the remaining grid.

4 Object Recognition Experiments

In this paper, Gabor wavelet filters $G_{\vec{\psi}}$ are defined by 7 logarithmically spaced center frequencies (filter bands) and 8 orientations for each filter band. Thus, we sample the frequency domain by 56 bandpass spectral channels. These filters are indexed by $k \in \{0, \ldots, 6\}$ and $l \in \{0, \ldots, 7\}$ Other parameters in (2) are chosen as :

$$\rho = \sqrt{2}, \quad \omega_0 = \frac{\pi}{16}, \quad \theta_0 = \frac{\pi}{8} \text{ and } \lambda = \pi/4,$$

The annealing temperature T is set between 3 and 5, the elastic parameter μ is set between 0.8 and 2.5, such that small number allows more grid deformation, and larger number allows less grid deformation. The cooling factor β is generally set to 1.15.

Example of Single Object

Figure 6 shows an example where object undergoes scale, aspect and signature variations and different object signatures (Figure 6). In this experiment, the distortion values (with respect to model) correspond to 105m in viewing distance, 11° in depression angle, and 52° in aspect angle.

When object scale is not a power of the center frequency of the Gabor wavelet representation, two scale factors will be used. The model Gabor probes will be scaled according to the closest power of the center frequency, and the edge of the Gabor grid will be scaled using the exact object scales. The flexible matching and the Gabor wavelet representation is invariant to such distortions. To find the correct object aspect, matching results are evaluated based on the criteria discussed earlier, and the ranks for matching are shown in Figure 6.

(a) Model

(b) Object 1   (c) Object 2   (d) Object 2

(e) Rank 2   (f) Rank 1   (g) Rank 3
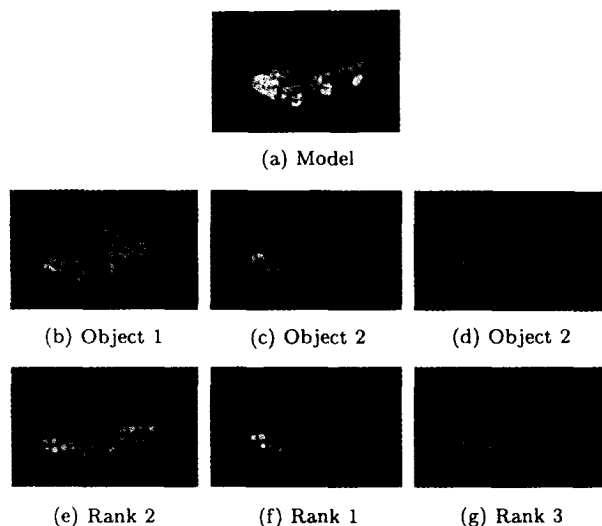
Figure 6: An object model is matched with three objects having scale, aspect variations, and different signatures. The size of the images is 300x200. They are taken as the region of interest from original images of size 512x512.

Examples of Multiple Objects

Four object classes with a total of 16 object aspects are extracted from the second generation infrared images, as the regions of interest of the object for recognition. A successful recognition rate of 83% was achieved for 12 experiments. The error occurred in object aspects having severe aspect and signature distortions from the given object model. Only the first two evaluation criteria defined earlier are used to obtain the matching results. Gabor phased-based evaluation is not used since the interior structure of the object is quite cold and phase measured at boundary points suffer wrap-around errors.

Recognizing occluded objects

An occluded object is selected from the second generation infrared image database which is identified as a ASTRO shown in Figure 7. Although the grid in the initial matching results are not collapsed in this example, the similarities of those grid nodes which matched with background clutter are relatively low with respect to the nodes which matched with the non-occluded part of the object. These randomly matched nodes are detected and removed from further consideration. The matching results which include both the initial matching and the repaired ones are presented. To illustrate the performance of matching under distortion, the edge boundaries of the object model are back projected onto the occluded object using the repaired distorted Gabor grid (Figure 7).

5 Conclusions

In this work, we have shown that the multi-scale Gabor wavelet representation and flexible matching technique are robust methods for object recognition under real-world conditions. The successes of this work lies in the following aspects. (a) Our flexible matching approach can tolerate variations of

(a) object   (b) Model   (c) Result 1

(d) Result 2   (e) Model   (f) Projection
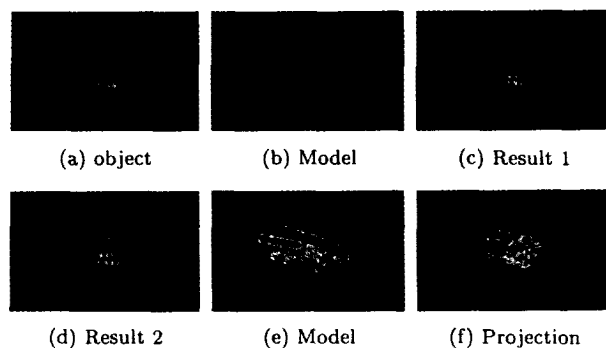
Figure 7: Matching with occluded object

up to 20° in depression angle and 22.5° in aspect. (b) The single scale multi-resolution representation of a model can be used to recognize objects with the size varying from 256 to 16k pixels, and a temperature varying from $12°C$ to $26°C$. (c) The grid erosion (repairing) can be used to recognize an object having up to 50% occlusion.

References

[1] B. Bhanu, R.N. Braithwaite, R. Dutta, S. Rong, A. Forslund, J.P. Djamdji, J.H. Yi, and X. Wu. Gabor wavelets for automatic target detection and recognition. Quarterly report to arpa, U.C. Riverside, January 1995.

[2] J.G. Daugman. Complete discrete 2-D Gabor transforms by neural networks for image analysis and compression. IEEE Trans. on Acoustics, Speech, and Signal Processing, 36(7):1169–1179, 1988.

[3] D.J. Fleet, A.D. Jepson, and M.R. Jenkin. Phase-based disparity measurement. Computer Vision, Graphics, and Image Processing: Image Understanding, 53(2):198–210, 1991.

[4] M. Lades, J.C. Vorbrüggen, J. Buhmann, J. Lange, C.v.d. Malsburg, R.P. Würtz, and W. Konen. Distortion invariant object recognition in the dynamic link architecture. IEEE Trans. Computers, 42(3):300–311, March 1993.

[5] S.G. Mallat. A theory for multiresolution signal decomposition: the Wavelet representation. IEEE Trans. Pattern Analysis and Machine Intelligence, 11:674–693, 1989.

[6] T.D. Sanger. Stereo disparity using Gabor filters. Biological Cybernetics, 59:405–418, 1988.